Acta Mech 226, 2379–2391 (2015)
DOI 10.1007/s00707-015-1329-z

ORIGINAL PAPER

V. Govorukha · M. Kamlah · A. Sheveleva

# Influence of concentrated loading on opening of an interface crack between piezoelectric materials in a compressive field

Received: 6 October 2014 / Revised: 23 January 2015 / Published online: 12 March 2015


**Abstract** A plane problem for an electrically permeable tunnel crack between two piezoelectric half-spaces under concentrated loading applied to the crack faces and remote mixed-mode loading is studied. The elastic displacement and potential jumps as well as the stresses and electrical displacement along the interface are represented via sectionally holomorphic vector functions. At the crack tip, we assume closed crack faces with frictionless contact at the crack tip. The problem is reduced to combined Dirichlet–Riemann boundary value problems that are solved analytically. From these solutions, clear analytical expressions for characteristics of the electromechanical field at the interface are derived. A transcendental equation, which determines the point of separation of the open and closed section of the crack, is found. The stress intensity factors at the crack tip and the energy release rate are calculated. The influence of the magnitude and the locations of the applied concentrated loading upon the contact zone length and the associated fracture mechanical parameters is considered.

## 1 Introduction

Due to the well-known mechanical–electrical coupling in piezoelectric ceramics, these kinds of materials are found to have wide technological applications such as transducers, sensors and actuators. As with most ceramic materials, a significant disadvantage of piezoelectric ceramics is their brittleness. Stress concentrations at defects or inhomogeneities, such as cracks, cavities, or particles in a piezoelectric material, can contribute to critical crack growth and subsequent mechanical failure or dielectric breakdown. Therefore, it is important to understand and to be able to analyze the fracture characteristics of piezoelectric materials so that reliable service life predictions of the pertinent devices can be conducted.

The problem of a crack in a homogeneous piezoelectric material has received much attention in the literature and has been studied intensively [1–7]. On the other hand, the problem of an interface crack in a piezoelectric bimaterial, in spite of its importance, has not obtained due attention in the literature because of its complexity. The first attempt to analyze the interface crack problem from a fracture mechanics point of view can be

V. Govorukha · A. Sheveleva (✉)
Department of Computational Mathematics, Dniepropetrovsk National University, Gagarin Av. 72,
Dniepropetrovsk 49010, Ukraine
E-mail: allasheveleva@i.ua

V. Govorukha
E-mail: govorukhavb@yahoo.com

M. Kamlah
Institute of Applied Materials, Karlsruhe Institute of Technology, Hermann-von-Helmholtz-Platz 1,
76344 Eggenstein-Leopoldshafen, Germany
E-mail: Marc.kamlah@kit.edu

found in [8], where a finite crack at the interface of a piezoelectric material and a conductor subjected to a far-field uniform tension is considered. Later, Kuo and Barnet [9], as well as Suo et al. [10] and Gao et al. [11] investigated the problem of an interface crack between dissimilar anisotropic piezoelectric materials by introducing the one-complex variable approach that simplified the calculations significantly. Weight function analysis for interface cracks in dissimilar anisotropic piezoelectric materials has been proposed and investigated by Ma and Chen [12]. Stress singularities of an interface crack in a piezoelectric bimaterial have been explicitly studied in [13,14] with respect to various boundary conditions on the crack faces. Analytical investigations of near-tip fields in dissimilar piezoelectric media have been performed in [15,16]. A crack terminating at a piezoelectric bimaterial interface was studied in [17].

It is worth to note that all mentioned results were performed within the framework of the so-called classical interface crack model [18]. This model assumes that the crack is completely open and usually leads to an oscillating singularity at the crack tips and physically unreal overlapping of the crack faces. To eliminate this phenomenon, a contact zone model for a crack between isotropic materials was suggested by Comninou [19] and further developed by Atkinson [20], Simonov [21], Gautesen and Dundurs [22], Loboda [23] and others. The contact zone approach was applied to interface cracks in linear thermopiezoelectric media by Qin and Mai [24], in magnetoelectroelastic materials by Herrmann et al. [25], Feng et al. [26], and for an electrically permeable, impermeable and limited permeable crack in piezoelectric materials by Herrmann and Loboda [27], Herrmann et al. [28] and Govorukha and Kamlah [29], respectively.

Most of the investigations related to an interface crack were performed for either tensile or simultaneous tensile-shear loading acting far away from the crack. However, sometimes piezoelectric bimaterials possessing interface cracks work under remote compression and shear fields together with concentrated loading on the crack faces caused by a disjoining action in the crack region. Under pure compressive loading, the cracks in homogeneous materials are usually closed, but interface cracks can be partially open in the presence of additional shear loading. For isotropic bimaterials, this possibility was shown by Comninou and Schmueser [30] using numerical methods and by Atkinson [20], Simonov [21] and Gautesen and Dundurs [22] in an analytical way. The influence of a concentrated load at the crack faces in a homogeneous piezoelectric material has been studied by Chen and Han [31] for a finite crack and by Hou et al. [32] for a circular crack. The interface cracks with contact zone between two different piezoelectric materials under distributed far-field loading have been studied in [27–29]. However, to the best of the authors' knowledge, the combined effect of a concentrated crack face load and remote mixed-mode loading upon an interface crack in a piezoelectric bimaterial has not been considered yet. As a matter of fact, this combination of the loads leads to the prediction of a peculiar effect of the crack tip opening, which is worth being investigated theoretically from a fundamental point of view.

In the present paper, a plane problem for an electrically permeable tunnel crack between two piezoelectric half-spaces is considered with taking into account the mechanical contact of the crack faces. Exact analytical solutions for such crack under the action of concentrated crack face loads and uniformly distributed remote loads are obtained. The method used in the paper is valid for arbitrary loading conditions, but in this paper the main attention is devoted to the case of compressive remote loading to investigate in particular the possibility of crack opening under such loading.

## 2 General solution for transversely isotropic piezoelectric media

In the absence of body forces and free charges, the governing equations for a linear piezoelectric solid can be expressed in Cartesian coordinates $x_i$ $(i = 1, 2, 3)$ as [33]

$$\sigma_{ij,j} = 0, \quad D_{i,i} = 0, \tag{1}$$

$$\sigma_{ij} = c_{ijkl}\gamma_{kl} - e_{kij}E_k, \quad D_i = e_{ikl}\gamma_{kl} + \varepsilon_{ik}E_k, \tag{2}$$

$$\gamma_{ij} = (u_{i,j} + u_{j,i})/2, \quad E_i = -\varphi_{,i} \tag{3}$$

where a comma indicates partial differentiation with regard to the respective coordinate; $\varphi$ is the electric potential; $u_i$, $\sigma_{ij}$, $\gamma_{ij}$, $E_i$ and $D_i$ are the components of elastic displacements, stress, strain, electric field and electric displacement, respectively, while $c_{ijkl}$, $e_{ijk}$ and $\varepsilon_{ij}$ are the elastic, piezoelectric and dielectric constants. The subscripts in (1)-(3) range from 1 to 3, and Einstein's summation convention is used in (1), (2).

For a two-dimensional problem in the $(x_1, x_3)$-plane, a general solution of (1)-(3) can be given by Suo et al. [10],

$$\mathbf{V} = \mathbf{A}\mathbf{f}(z) + \overline{\mathbf{A}}\overline{\mathbf{f}}(\overline{z}), \tag{4}$$

$$\mathbf{t} = \mathbf{B}\mathbf{f}'(z) + \overline{\mathbf{B}}\overline{\mathbf{f}}'(\overline{z}), \tag{5}$$

where $\mathbf{V} = [u_1, u_2, u_3, \varphi]^T$, $\mathbf{t} = [\sigma_{13}, \sigma_{23}, \sigma_{33}, D_3]^T$ and $\mathbf{f}(z)$ consists of four analytic functions of the respective variables $z_\alpha = x_1 + p_\alpha x_3 (\alpha = 1, 2, 3, 4)$ as

$$\mathbf{f}(z) = [f_1(z_1), f_2(z_2), f_3(z_3), f_4(z_4)]^T .$$

Matrices $\mathbf{A}$ and $\mathbf{B}$ are determined from an eigenvalue problem [10] and are defined by the material constants; $p_\alpha$ are four distinct eigenvalues with positive imaginary parts.

Consider a bimaterial composed of two different piezoelectric half-planes $x_3 > 0$ and $x_3 < 0$, respectively. In this case according to (4), (5), the solutions of (1)-(3) can be written for each domain in the form

$$\mathbf{V}^{(j)} = \mathbf{A}^{(j)}\mathbf{f}^{(j)}(z) + \overline{\mathbf{A}}^{(j)}\overline{\mathbf{f}}^{(j)}(\overline{z}), \tag{6}$$

$$\mathbf{t}^{(j)} = \mathbf{B}^{(j)}\mathbf{f}'^{(j)}(z) + \overline{\mathbf{B}}^{(j)}\overline{\mathbf{f}}'^{(j)}(\overline{z}) \tag{7}$$

where $j = 1$ stands for $x_3 > 0$ and $j = 2$ for $x_3 < 0$; the vector functions $\mathbf{f}^{(1)}(z)$ and $\mathbf{f}^{(2)}(z)$ are analytic in the upper $(x_3 > 0)$ and the lower $(x_3 < 0)$ half-planes, respectively.

Furthermore, an analysis similar to [27] leads by means of the formulas (6), (7) to the expressions

$$\left\langle \mathbf{V}'(x_1) \right\rangle = \mathbf{D}\mathbf{f}'^{(1)}(x_1) + \overline{\mathbf{D}}\overline{\mathbf{f}}'^{(1)}(x_1),$$

$$\mathbf{t}(x_1, 0) = \mathbf{B}^{(1)}\mathbf{f}'^{(1)}(x_1) + \overline{\mathbf{B}}^{(1)}\overline{\mathbf{f}}'^{(1)}(x_1)$$

where $\mathbf{D} = \mathbf{A}^{(1)} - \overline{\mathbf{A}}^{(2)} \left(\overline{\mathbf{B}}^{(2)}\right)^{-1} \mathbf{B}^{(1)}$. Here and afterwards, the brackets $\langle ... \rangle$ denote the jump of the corresponding function over the material interface, i.e., $\left\langle \mathbf{V}'(x_1) \right\rangle = \mathbf{V}'^{(1)}(x_1, 0) - \mathbf{V}'^{(2)}(x_1, 0)$.

Introducing the vector function

$$\mathbf{W}(z) = \begin{cases} \mathbf{D}\mathbf{f}'^{(1)}(z) & \text{for } x_3 > 0, \\ -\overline{\mathbf{D}}\overline{\mathbf{f}}'^{(1)}(z) & \text{for } x_3 < 0, \end{cases}$$

one obtains

$$\left\langle \mathbf{V}'(x_1) \right\rangle = \mathbf{W}^+(x_1) - \mathbf{W}^-(x_1), \tag{8}$$

$$\mathbf{t}(x_1,\ 0) = \mathbf{G}\mathbf{W}^+(x_1) - \overline{\mathbf{G}}\mathbf{W}^-(x_1) \tag{9}$$

where $\mathbf{G} = \mathbf{B}^{(1)}\mathbf{D}^{-1}$, $\mathbf{W}^{\pm}(x_1) = \mathbf{W}(x_1 \pm i0)$.

It follows from (8) that the vector function $\mathbf{W}(z) = [W_1(z), W_2(z), W_3(z), W_4(z)]^T$ is analytical on the whole complex plane, including the bonded parts of the material interface. Moreover, the matrix $\mathbf{G}$ and the vector function $\mathbf{W}(z)$ are related to the matrix $\mathbf{H}$ and the vector function $\mathbf{h}(z)$ of the paper by Suo et al. [10] according to $\mathbf{H} = i\mathbf{G}^{-1}$, $\mathbf{W}(z) = -i\mathbf{H}\mathbf{h}(z)$, respectively.

We will focus our attention on a transversely isotropic piezoelectric material of the symmetry class 6 mm poled in the $x_3$-direction, which has an essential practical significance. In this case, the matrix $\mathbf{G}$ has the following structure:

$$\mathbf{G} = \begin{bmatrix} ig_{11} & 0 & g_{13} & g_{14} \\ 0 & ig_{22} & 0 & 0 \\ g_{31} & 0 & ig_{33} & ig_{34} \\ g_{41} & 0 & ig_{43} & ig_{44} \end{bmatrix} \tag{10}$$

where all $g_{ij}$ are real and the relations $g_{31} = -g_{13},\ g_{41} = -g_{14},\ g_{43} = g_{34}$ hold true.

The analysis of the matrix (10) shows that the stress–strain state in this case can be decoupled into an in-plane and an out-of-plane problem. Because the out-of-plane problem is relatively simple, the main attention will be devoted to the in-plane problem that is characterized by the displacements $u_1$, $u_3$ and the electric potential $\varphi$.

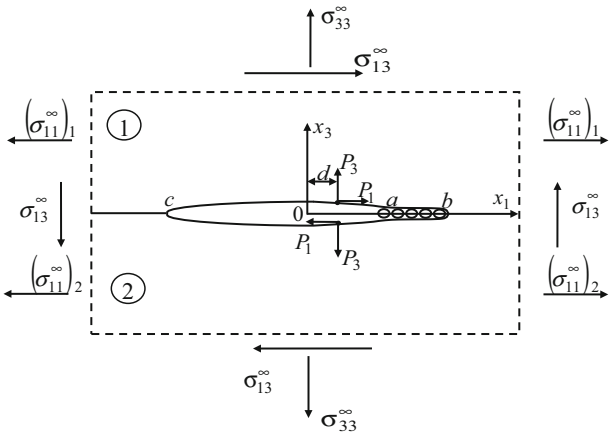


**Fig. 1** A crack between two piezoelectric materials with open zone $(c, a)$ and closed one $(a, b)$

## 3 Formulation of the problem and derivation of the basic relation

Consider a tunnel interface crack situated in the region $c < x_1 < b$, $x_3 = 0$ between two piezoelectric half-spaces $x_3 > 0$ (with matrices $c_{ijkl}^{(1)}$, $e_{ijk}^{(1)}$ and $\varepsilon_{ij}^{(1)}$ of the physical properties) and $x_3 < 0$ (with matrices $c_{ijkl}^{(2)}$, $e_{ijk}^{(2)}$ and $\varepsilon_{ij}^{(2)}$). It is assumed that the direction of the polarization of both materials is orthogonal to the crack faces. The crack is loaded by the concentrated traction $(P_1, P_3)$ applied to its faces at the prescribed point $(d, 0)$ as well as by far-field uniform stresses $\sigma_{33}^{(j)} = \sigma_{33}^{\infty}, \sigma_{13}^{(j)} = \sigma_{13}^{\infty}$ and $\sigma_{11}^{(j)} = \left(\sigma_{11}^{\infty}\right)_j \quad (j = 1, 2)$, which satisfy the continuity conditions at the interface. Since the load does not depend on coordinate $x_2$, a plane strain problem in the $(x_1, x_3)$-plane can be considered (Fig. 1).

Following Comninou [19], we introduce a frictionless contact zone $a < x_1 < b$ at the right crack tip to avoid an oscillating singularity, where the position of the point $a$ is chosen arbitrarily for the time being. For such an arbitrary position of point $a$, we have an artificial contact zone model, which is not physically justified, but from this model the specific value of $a$ for the contact zone length in the sense of Comninou will be found. The corresponding conditions for a realistic contact zone length will be formulated in Sect. 6.

The electrical potential is assumed to be continuous across the whole interface. This type of condition of continuity is completely justified for a crack filled with a conducting fluid. Furthermore, according to Gao and Fan [5], even for cracks filled by air such a condition is more realistic than the condition of electrically insulated crack faces. Thus the continuity and boundary conditions at the interface $x_3 = 0$ are the following:

$$\langle \sigma_{33} \rangle = 0, \quad \langle \sigma_{13} \rangle = 0, \quad \langle \varphi \rangle = 0, \quad \langle D_3 \rangle = 0, \quad x_1 \in (-\infty, \infty); \tag{11}$$

$$\langle u_1 \rangle = 0, \quad \langle u_3 \rangle = 0, \quad x_1 \notin (c, b); \tag{12}$$

$$\sigma_{33}^{\pm} = -P_3 \delta(x_1 - d), \quad \sigma_{13}^{\pm} = -P_1 \delta(x_1 - d), \quad x_1 \in (c, a), \tag{13}$$

$$\langle u_3 \rangle = 0, \quad \sigma_{13}^{\pm} = 0, \quad x_1 \in (a, b) \tag{14}$$

where the superscripts + and – refer to the upper and lower boundary values, respectively, and $\delta(x_1 - d)$ is Dirac's delta-function.

Using the expressions (8), (9), taking into account that $\langle \varphi \rangle = 0$ for $x_1 \in (-\infty, \infty)$ and performing the analysis similar to Herrmann and Loboda [27], one arrives at the equations

$$\sigma_{33}(x_1, 0) + im\sigma_{13}(x_1, 0) = t[F^+(x_1) + \gamma F^-(x_1)], \tag{15}$$

$$\left\langle u_1'(x_1) \right\rangle + is \left\langle u_3'(x_1) \right\rangle = F^+(x_1) - F^-(x_1) \tag{16}$$

where

$$s = \frac{g_{33} + mg_{13}}{t}, \quad \gamma = -\frac{g_{31} + mg_{11}}{t}, \quad t = g_{31} - mg_{11}, \quad m = -\sqrt{\frac{g_{33}}{g_{11}}}.$$

It is worth to note that the constants $m, s, t$ and $\gamma$ have real values for certain classes of piezoelectric ceramics. Besides, the unknown function $F(z)$ is analytic in the whole plane including the bonded parts of the material interface.

The above-mentioned formulations can be used to derive the solution for an interface crack in a piezoelectric bimaterial under combined loadings as shown in Fig. 1. Because of the linearity of the formulated problem, the solution of this problem requires the solution of the following problems:

(a) solution for an interface crack under concentrated loading;
(b) solution for an interface crack under remote mixed-mode loading.

The superposition of the above solutions gives an analytical solution of the considered problem.

## 4 An interface crack under a concentrated loading

Consider an interface crack $(c, b)$ with a frictionless contact zone $(a, b)$ in a piezoelectric bimaterial plane (Fig. 1) under the action of a pure concentrated loading $(P_1, P_3)$ applied at the point $(d, 0)$ of both faces of a crack.

The satisfaction of the conditions (13), (14) by means of the expressions (15), (16) leads to the inhomogeneous combined Dirichlet–Riemann boundary value problem

$$F^+(x_1) + \gamma F^-(x_1) = g(x_1), \quad x_1 \in (c, a), \tag{17}$$

$$\text{Im } F^{\pm}(x_1) = 0, \quad x_1 \in (a, b), \tag{18}$$

with respect to the sectionally holomorphic function $F(z)$, where $g(x_1) = -t^{-1}(P_3 + imP_1)\delta(x_1 - d)$.

This problem is much more complicated and less studied than the Riemann–Hilbert problem. A solution of a homogeneous problem associated with (17), (18) was found and applied to the analysis of a rigid stamp in [34]. For the problem of an interface crack, the solution of the homogenous problem was developed by Loboda [23]. Let us now consider the solution of the inhomogeneous problem (17), (18). Following Nahmein and Nuller [34] and denoting by

$$X(z) = \frac{e^{i\phi(z)}}{\sqrt{(z-c)(z-a)}},$$

with

$$\phi(z) = 2\varepsilon \ln \frac{\sqrt{(b-a)(z-c)}}{\sqrt{(b-c)(z-a)} + \sqrt{(a-c)(z-b)}}, \quad \varepsilon = \frac{1}{2\pi} \ln \gamma,$$

a particular solution of a homogeneous problem associated with (17), (18), Eq. (17) can be written as

$$\frac{F^+(x_1)}{X^+(x_1)} - \frac{F^-(x_1)}{X^-(x_1)} = \frac{g(x_1)}{X^+(x_1)}, \quad x_1 \in (c,\ a). \tag{19}$$

A solution of Eq. (19) is [35]

$$\frac{F(z)}{X(z)} = \omega_1(z) + \omega_2(z) \tag{20}$$

where $\omega_1(z) = \frac{1}{2\pi i} \int\limits_c^a \frac{g(t)\mathrm{d}t}{X^+(t)(t-z)}$ and $\omega_2(z)$ is an arbitrary analytic function on $x_1 \in (c, a)$. Taking into account that $X^{\pm}(x_1)$ is real on $x_1 \in (c, a)$, Eq. (18) leads to

$$\text{Im}\omega_2^{\pm}(x_1) = H^{\pm}(x_1), \quad x_1 \in (a, b) \tag{21}$$

where $H^{\pm}(x_1) = -\text{Im } \omega_1^{\pm}(x_1)$. Equation (21) can be written as

$$\text{Re}[-i\omega_2^{\pm}(x_1)] = H^{\pm}(x_1), \quad x_1 \in (a, b). \tag{22}$$

Using a solution of the Dirichlet problem (22) given by the formula (46.25) of [35], the function $\omega_2(z)$ can be written as

$$\omega_2(z) = \frac{Y(z)}{2\pi} \int_a^b \frac{H^+(t) + H^-(t)}{Y^+(t)(t-z)} \mathrm{d}t + \frac{1}{2\pi} \int_a^b \frac{H^+(t) - H^-(t)}{t-z} \mathrm{d}t \tag{23}$$

where $Y(z) = \sqrt{\frac{z-a}{z-b}}$.

Transforming (23) with help of the relations [35],

$$\int_a^b \frac{\mathrm{d}t}{Y^+(t)(t-z)(d-t)} = \frac{\pi i}{d-z} \left[ \frac{1}{Y(z)} - \frac{1}{Y(d)} \right],$$

we obtain

$$\omega_2(z) = \frac{i\ \mathrm{Im}(I_0)}{z-d} \left[ 1 - \frac{Y(z)}{Y(d)} \right]$$

where

$$I_0 = -\frac{P_3 + imP_1}{2\pi i t X^+(d)}.$$

Using formula (20), the solution of the inhomogeneous problem (17), (18) for trivial values of $F(z)$ at infinity can be written in the form

$$F(z) = \frac{X(z)}{d-z} \left[ \mathrm{Re}(I_0) + i\mathrm{Im}(I_0) \frac{Y(z)}{Y(d)} \right]. \tag{24}$$

The obtained solution and the formula (16) lead to the following expressions for the derivatives of the displacement jumps for $x_1 \in (c, a)$:

$$\left\langle u_1'(x_1) \right\rangle + is \left\langle u_3'(x_1) \right\rangle = \frac{(1+\gamma) e^{i\phi^*(x_1)}}{i(d-x_1)\sqrt{\gamma(x_1-c)(a-x_1)}} \left[ \mathrm{Re}(I_0) + i\mathrm{Im}(I_0) \frac{Y(x_1)}{Y(d)} \right]. \tag{25}$$

Similarly it follows from Eqs. (15), (16) and (24) that in the contact zone $x_1 \in (a, b)$

$$\begin{aligned} \sigma_{33}(x_1, 0) = {} & \frac{t(1+\gamma)}{(d-x_1)\sqrt{(x_1-c)(x_1-a)}} \left\{ \mathrm{Re}(I_0) \left[ \cosh\tilde{\phi}(x_1) + \frac{1-\gamma}{1+\gamma} \sinh\tilde{\phi}(x_1) \right] \right. \\ & \left. + \frac{\mathrm{Im}(I_0)}{Y(d)} \sqrt{\frac{x_1-a}{b-x_1}} \left[ \sinh\tilde{\phi}(x_1) + \frac{1-\gamma}{1+\gamma} \cosh\tilde{\phi}(x_1) \right] \right\}, \end{aligned} \tag{26}$$

$$\left\langle u_1'(x_1) \right\rangle = \frac{2}{(d-x_1)\sqrt{(x_1-c)(x_1-a)}} \left\{ \mathrm{Re}(I_0) \sinh\tilde{\phi}(x_1) + \frac{\mathrm{Im}(I_0)}{Y(d)} \sqrt{\frac{x_1-a}{b-x_1}} \cosh\tilde{\phi}(x_1) \right\}, \tag{27}$$

while for $x_1 > b$

$$\sigma_{33}(x_1, 0) + im\sigma_{13}(x_1, 0) = \frac{t(1+\gamma)X(x_1)}{d-x_1} \left[ \mathrm{Re}(I_0) + i\mathrm{Im}(I_0) \frac{Y(x_1)}{Y(d)} \right] \tag{28}$$

where

$$\phi^*(x_1) = 2\varepsilon \ln \frac{\sqrt{(b-a)(x_1-c)}}{\sqrt{(b-c)(a-x_1)} + \sqrt{(a-c)(b-x_1)}}, \quad \tilde{\phi}(x_1) = 2\varepsilon \tan^{-1} \sqrt{\frac{(a-c)(b-x_1)}{(b-c)(x_1-a)}}.$$

Once the function $F(z)$ has been found, the explicit expressions for normal component of the electric displacement at the material interface can be derived from Eqs. (8) and (9) as

$$D_3(x_1, 0) = \frac{g_{41}g_{33} - g_{43}g_{31}}{g_{33}} \left\langle u_1'(x_1) \right\rangle + \frac{g_{43}}{g_{33}} \sigma_{33}(x_1, 0), \quad \text{for } x_1 \in (c, b);$$

$$D_3(x_1, 0) = \frac{g_{43}}{g_{33}} \sigma_{33}(x_1, 0), \quad x_1 > b.$$

## 5 An interface crack under a remote mixed-mode loading

Consider now again the finite length interface crack $(c, b)$ with a frictionless contact zone $(a, b)$ depicted in Fig. 1, and assume that the concentrated loading is equal to zero, and a uniform mixed-mode loading $\sigma_{33}^{(j)} = \sigma_{33}^{\infty}$, $\sigma_{13}^{(j)} = \sigma_{13}^{\infty}$ and $\sigma_{11}^{(j)} = \left(\sigma_{11}^{\infty}\right)_j$ $(j = 1, 2)$, which satisfies the continuity conditions at the interface, is prescribed at infinity.

The interface conditions of the problem coincide with Eqs. (11)–(14) provided $P_1 = P_3 = 0$ is valid, and the following homogeneous combined Dirichlet–Riemann boundary value problem:

$$F^+(x_1) + \gamma F^-(x_1) = 0, \quad x_1 \in (c, a), \tag{29}$$

$$\operatorname{Im} F^{\pm}(x_1) = 0, \quad x_1 \in (a, b), \tag{30}$$

for the sectionally holomorphic function $F(z)$ holds true.

By using Eq. (15) and the prescribed remote loads, the conditions at infinity for the function $F(z)$can be written as

$$F(z)|_{z\to\infty} = \frac{\sigma_{33}^{\infty} + im\sigma_{13}^{\infty}}{t(1+\gamma)}. \tag{31}$$

The general solution of the problem (29), (30) can be represented according to [23] in the form

$$F(z) = P(z)X_1(z) + Q(z)X_2(z) \tag{32}$$

where

$$X_1(z) = \frac{ie^{i\phi(z)}}{\sqrt{(z-c)(z-b)}}, \quad X_2(z) = \frac{e^{i\phi(z)}}{\sqrt{(z-c)(z-a)}},$$
$$P(z) = C_0 + C_1 z, \quad Q(z) = D_0 + D_1 z.$$

The real coefficients $C_0$, $C_1$, $D_0$, $D_1$ can be found from the conditions (31) at infinity in the form

$$C_1 = \frac{1}{t(1+\gamma)}\left(m\sigma_{13}^{\infty}\cos\beta - \sigma_{33}^{\infty}\sin\beta\right), \quad D_1 = \frac{1}{t(1+\gamma)}\left(m\sigma_{13}^{\infty}\sin\beta + \sigma_{33}^{\infty}\cos\beta\right),$$
$$C_0 = -\beta_1 D_1 - \frac{c+b}{2}C_1, \quad D_0 = \beta_1 C_1 - \frac{c+a}{2}D_1$$

where

$$\beta = \varepsilon \ln\frac{\lambda}{(1+\sqrt{1-\lambda})^2}, \quad \beta_1 = \varepsilon\sqrt{(a-c)(b-c)}.$$

The parameter $\lambda = \frac{b-a}{b-c}$ defines the relative length of the contact zone of the crack faces and will be found later.

Substituting the formula (32) into (15), (16) and taking into account that $F^+(x_1) = F^-(x_1)$ for $x_1 > b$ and $F^-(x_1) = -F^+(x_1)/\gamma$ for $x_1 \in (c, a)$, the following expressions are obtained for the stresses and the derivatives of the displacement jumps at the material interface for $x_1 > b$:

$$\sigma_{33}(x_1, 0) + im\sigma_{13}(x_1, 0) = \frac{t(1+\gamma)e^{i\phi(x_1)}}{\sqrt{x_1 - c}}\left[\frac{Q(x_1)}{\sqrt{x_1 - a}} + i\frac{P(x_1)}{\sqrt{x_1 - b}}\right], \tag{33}$$

$$D_3(x_1, 0) = \frac{g_{43}}{g_{33}}\left[\sigma_{33}(x_1, 0) - \sigma_{33}^{\infty}\right],$$

for $x_1 \in (c, a)$:

$$\left\langle u_1'(x_1)\right\rangle + is\left\langle u_3'(x_1)\right\rangle = \frac{(1+\gamma)e^{i\phi^*(x_1)}}{\sqrt{\gamma(x_1 - c)}}\left[\frac{P(x_1)}{\sqrt{b - x_1}} - i\frac{Q(x_1)}{\sqrt{a - x_1}}\right], \tag{34}$$

$$D_3(x_1, 0) = \frac{g_{41}g_{33} - g_{43}g_{31}}{g_{33}}\left\langle u_1'(x_1)\right\rangle - \frac{g_{43}}{g_{33}}\sigma_{33}^{\infty},$$

for $x_1 \in (a, b)$:

$$\sigma_{33}(x_1, 0) = \frac{t(1+\gamma)P(x_1)}{\sqrt{(x_1 - c)(b - x_1)}} \left[ \sinh \tilde{\phi}(x_1) + \frac{1-\gamma}{1+\gamma} \cosh \tilde{\phi}(x_1) \right] + \frac{t(1+\gamma)Q(x_1)}{\sqrt{(x_1 - c)(x_1 - a)}} \left[ \cosh \tilde{\phi}(x_1) + \frac{1-\gamma}{1+\gamma} \sinh \tilde{\phi}(x_1) \right], \tag{35}$$

$$\left\langle u_1'(x_1) \right\rangle = \frac{2}{\sqrt{x_1 - c}} \left[ \frac{P(x_1)}{\sqrt{b - x_1}} \cosh \tilde{\phi}(x_1) + \frac{Q(x_1)}{\sqrt{x_1 - a}} \sinh \tilde{\phi}(x_1) \right], \tag{36}$$

$$D_3(x_1, 0) = \frac{g_{41}g_{33} - g_{43}g_{31}}{g_{33}} \left\langle u_1'(x_1) \right\rangle + \frac{g_{43}}{g_{33}} \left[ \sigma_{33}(x_1, 0) - \sigma_{33}^{\infty} \right].$$

## 6 Behavior of the solution at singular points and the determination of the contact zone length in the sense of Comninou

In this section, the behavior of the stresses as well as the displacement jumps at the right crack tip and at the ends of the contact zone is considered. At the left crack tip, there is an oscillating singularity considered in detail by Beom [13], and therefore, no special attention will be given to this point.

As it follows from the analysis of the formulas (28) and (33), the normal stress is limited for $x_1 \to b + 0$. On the other hand, the shear stress is singular for $x_1 \to b + 0$ as well as the normal stress for $x_1 \to a + 0$. The following stress intensity factors (SIFs) are introduced to characterize these singularities:

$$K_1 = \lim_{x_1 \to a+0} \sqrt{2\pi(x_1 - a)}\sigma_{33}(x_1, 0), \quad K_2 = \lim_{x_1 \to b+0} \sqrt{2\pi(x_1 - b)}\sigma_{13}(x_1, 0). \tag{37}$$

Using relations (26), (28) and (33), (35) leads to the expressions

$$K_1 = \frac{\sqrt{2\pi\gamma(b-c)}}{1+\lambda} \left\{ \sqrt{1-\lambda} \left( m\sigma_{13}^{\infty} \sin\beta + \sigma_{33}^{\infty} \cos\beta \right) + 2\varepsilon \left( m\sigma_{13}^{\infty} \cos\beta - \sigma_{33}^{\infty} \sin\beta \right) \right\} + \sqrt{\frac{2(1-\theta)}{\pi(b-c)(1-\lambda)(\theta-\lambda)}} \left\{ P_3 \cos\phi^*(d) + mP_1 \sin\phi^*(d) \right\}, \tag{38}$$

$$K_2 = \frac{1}{m}\sqrt{\frac{\pi(b-c)}{2}} \left\{ m\sigma_{13}^{\infty} \cos\beta - \sigma_{33}^{\infty} \sin\beta - 2\varepsilon\sqrt{1-\lambda} \left( m\sigma_{13}^{\infty} \sin\beta + \sigma_{33}^{\infty} \cos\beta \right) \right\} + \frac{1+\gamma}{m} \sqrt{\frac{1-\theta}{2\pi\gamma\theta(b-c)}} \left\{ mP_1 \cos\phi^*(d) - P_3 \sin\phi^*(d) \right\} \tag{39}$$

where

$$\theta = \frac{b-d}{b-c}.$$

The asymptotic behavior of the main characteristics of the electromechanical field at the points $a$ and $b$ can be represented via the SIFs in the form

$$\sigma_{33}(x_1, 0)|_{x_1 \to a+0} = \frac{K_1}{\sqrt{2\pi(x_1 - a)}}, \tag{40}$$

$$\sigma_{13}(x_1, 0)|_{x_1 \to b+0} = \frac{K_2}{\sqrt{2\pi(x_1 - b)}}, \tag{41}$$

$$\langle u_1(x_1) \rangle_{x_1 \to b-0} = -\frac{4mK_2}{t(1+\gamma)} \sqrt{\frac{b - x_1}{2\pi}}, \tag{42}$$

$$\langle u_3(x_1) \rangle_{x_1 \to a-0} = \frac{(1+\gamma)K_1}{st\gamma} \sqrt{\frac{a - x_1}{2\pi}}. \tag{43}$$

It follows from formulas (40)–(43) that the SIFs $K_1$ and $K_2$ completely define the behavior of the stresses as well as the displacement jumps at the right crack tip and at the ends of the contact zone.

The energy release rate (ERR) at the right crack tip can be represented in the form [33]

$$G = \lim_{\Delta l \to 0} \frac{1}{2\Delta l} \left\{ \int_a^{a+\Delta l} \sigma_{33}(\tau, 0)\, \langle u_3(\tau - \Delta l) \rangle\, d\tau + \int_b^{b+\Delta l} \sigma_{13}(\tau, 0)\, \langle u_1(\tau - \Delta l) \rangle\, d\tau \right\}. \tag{44}$$

It should be noted that the electrical part of the ERR is equal to zero because of the vanishing jump of the potential $\varphi$ along the whole interface. Substituting expressions (40)–(43) into (44), one gets after the evaluation of the integrals the expression

$$G = \frac{(1+\gamma)K_1^2}{8st\gamma} - \frac{mK_2^2}{2t(1+\gamma)}. \tag{45}$$

The obtained formulas are mathematically correct for any position of the point $a$, and the associated interface crack model was called an artificial contact zone model [27]. However, the obtained solution becomes physically correct only if the following additional conditions are satisfied:

$$\sigma_{33}(x_1, 0) \le 0 \quad \text{for } x_1 \in (a, b), \quad \langle u_3(x_1) \rangle \ge 0 \quad \text{for } x_1 \in (c, a). \tag{46}$$

These conditions mean that the normal stress in the contact region is compressive and that there is no overlapping of the crack faces. In this case, a contact zone in the sense of Comninou [19] is present at the crack tip.

An analytical analysis and numerical verifications show that inequalities (46) hold true if the crack closes smoothly at the point $a$, i.e.,

$$\lim_{x_1 \to a-0} \sqrt{a - x_1}\, \langle u_3'(x_1) \rangle = 0,$$

which is equivalent to the equation $K_1 = 0$. Due to the formulas (34) and (38), both of these equations can be written in the form of the transcendental equation

$$\frac{(b-c)\sqrt{\gamma}}{1+\lambda} \left\{ (1-\lambda) \left( m\sigma_{13}^{\infty} \sin\beta(\lambda) + \sigma_{33}^{\infty} \cos\beta(\lambda) \right) + 2\varepsilon\sqrt{1-\lambda} \left( m\sigma_{13}^{\infty} \cos\beta(\lambda) - \sigma_{33}^{\infty} \sin\beta(\lambda) \right) \right\}$$
$$+ \frac{1}{\pi} \sqrt{\frac{1-\theta}{\theta-\lambda}} \left\{ P_3 \cos\phi^*(\lambda) + mP_1 \sin\phi^*(\lambda) \right\} = 0, \tag{47}$$

with respect to $\lambda$, where

$$\beta(\lambda) = \varepsilon \ln \frac{\lambda}{(1+\sqrt{1-\lambda})^2}, \quad \phi^*(\lambda) = 2\varepsilon \ln \frac{\sqrt{\lambda(1-\theta)}}{\sqrt{\theta-\lambda} + \sqrt{\theta(1-\lambda)}}.$$

In general, Eq. (47) has to be solved numerically, and the maximum root $\lambda_0$ from the interval $(0, 1)$ should be taken, since this value is the contact zone length in the sense of Comninou. It should be noted that the second inequality of (46) cannot be satisfied in the zone of oscillation near the left crack tip. However, for the considered loadings, this zone is negligibly small, namely on the order of $10^{-8}$ as compared to the crack length. Thus, it does not influence the electromechanical characteristics at the right crack tip, which is the one we discuss in detail in the following.

## 7 Numerical results and discussion

The main attention of the following numerical analysis will be devoted to the combination of a concentrated crack face loading and remote distributed shear and compressive loading.

The numerical analysis has been performed for a bimaterial composed of piezoelectric ceramics PZT-5H (the upper material) and PZT-4 (the lower one). The material properties of these materials were taken from [36] and [3], respectively. The crack was situated in the segment $(-10, 10)$ mm. The position of the concentrated loading at the crack faces is defined by the parameter $\theta = \frac{b-d}{b-c}$. The remote shear stress was assumed to be equal $\sigma_{13}^{\infty} = -10$ MPa, and the normal stress was defined by the formula $\sigma_{33}^{\infty} = \omega\sigma_{13}^{\infty}$ with varying values of $\omega > 0$. We shall discuss the influence of the remote shear stress in the presence of a compressive normal stress and the

**Table 1** Relative contact zone length $\lambda_0$, the SIF $K_{20}$ and the ERR $G_0$ for different values of the normal stress $\sigma_{33}^{\infty}$

| $\omega$ | $\lambda_0$ | $\frac{K_{20}}{\sigma_{13}^{\infty}\sqrt{b-c}}$ | $-\frac{G_0 \cdot 10^3}{\sigma_{13}^{\infty}(b-c)}$ |
|---|---|---|---|
| 0.4 | 0.0904 | 1.281 | 0.1470 |
| 0.5 | 0.1810 | 1.277 | 0.1461 |
| 0.6 | 0.2543 | 1.274 | 0.1455 |
| 0.7 | 0.3126 | 1.272 | 0.1450 |
| 0.8 | 0.3596 | 1.270 | 0.1446 |
| 0.9 | 0.3981 | 1.269 | 0.1443 |
| 1.0 | 0.4304 | 1.267 | 0.1440 |

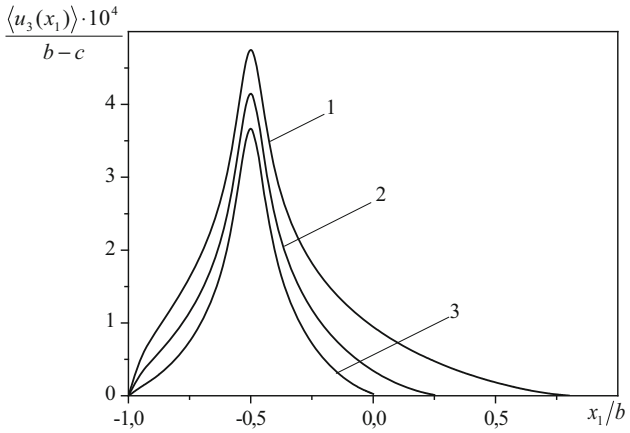


**Fig. 2** Crack opening for different values of applied loads $\sigma_{33}^{\infty}$

concentrated loading defined by the components $P_1$ and $P_3$. The specific values of remote and the concentrated loads are chosen to ensure the formation of a longer contact zone near the right crack tip. Furthermore, for a position $\theta$ of the concentrated load in the left half of the crack faces, the oscillating singularity at the left crack tip is assumed to have negligible influence on the fields at the right crack tip. In the opposite case, the problem can be reduced to the considered one by simple transposition of the upper and lower semi-infinite spaces.

The variation of the relative contact zone length $\lambda_0$, the SIF of the shear stress $K_{20} = K_2|_{\lambda=\lambda_0}$ at the right crack tip and the ERR $G_0 = G|_{\lambda=\lambda_0}$ with respect to normal load $\sigma_{33}^{\infty}$, defined by parameter $\omega$, for $P_1 = 0$, $P_3 = 2 \cdot 10^5$ N/m and $\theta = 0.75$ are presented in Table 1. It follows from the presented results that increasing $\omega$ leads to an increase in the relative contact zone length. In contrast to $\lambda_0$, the SIF $K_{20}$ and the ERR $G_0$ depend very slightly on the compressive loading $\sigma_{33}^{\infty}$. This means that the possibility of the crack propagation under remote compressive-shear loading is mostly defined by shear loading.

In Fig. 2, the graphs of the crack opening are presented for $P_1 = 0$, $P_3 = 2 \cdot 10^5$ N/m, $\theta = 0.75$ and different values of the normal compressive stress $\sigma_{33}^{\infty}$, defined by parameter $\omega = 0.4, 0.8, 1.2$ (line 1, 2, and 3, respectively). It is interesting to note that in spite of the normal stress being compressive, the crack opening remains positive not only in the immediate vicinity of the concentrated force, but in a much wider region that varies in dependence on the magnitude of the normal stress. Variations of the normal stress in the contact zone for the same external loads as in Fig. 2 are presented in Fig. 3. It is clearly seen from Figs. 2 and 3 that for all considered loadings the crack remains open in the intervals $(c, a)$ and the normal stress remains negative in the interval $(a, b)$. This means that the inequalities (46) are satisfied at any point of the crack region. It is worth to be mentioned as well that according to (26), (27) and (34), (35) $\langle u_3'(x_1)\rangle|_{x_1 \to a-0} \to 0$ and $\sigma_{33}(x_1, 0)|_{x_1 \to a+0} \to 0$, therefore, the crack is closed smoothly at the point $a$. This statement is evidently confirmed by Figs. 2 and 3.

The most dangerous stress component at the crack tip is the shear stress $\sigma_{13}(x_1, 0)$ in the ligament, i.e., in the neighborhood to the right of the crack tip $b$. The variations of this stress along the mentioned zone are presented in Fig. 4 for different shear loads $\sigma_{13}^{\infty} = -2.5$ MPa (line 1), $\sigma_{13}^{\infty} = -5$ MPa (line 2) and $\sigma_{13}^{\infty} = -10$ MPa (line 3) with fixed $\sigma_{33}^{\infty} = -5$ MPa and $P_1 = 0$, $P_3 = 2 \times 10^5$ N/m, $\theta = 0.75$. It is observed clearly from this figure that the absolute value of $\sigma_{13}(x_1, 0)$ increases with the increase in magnitude of the applied shear load.

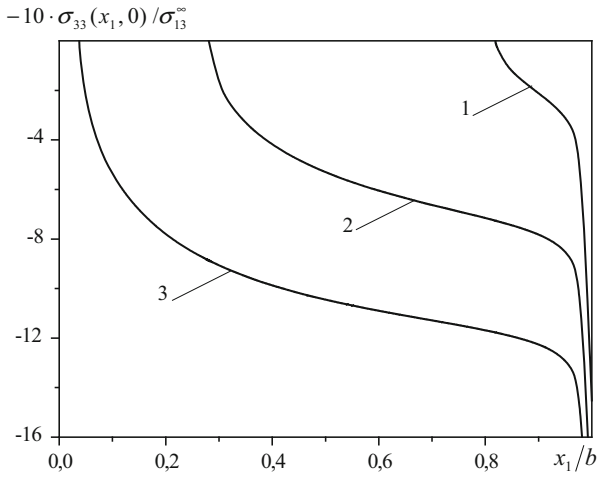


**Fig. 3** Normal stress $\sigma_{33}(x_1, 0)$ in the contact zone for different values of applied loads $\sigma_{33}^{\infty}$

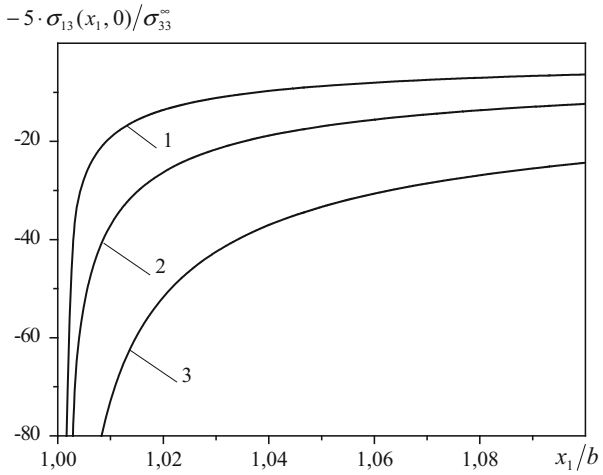


**Fig. 4** Shear stress $\sigma_{13}(x_1, 0)$ in the ligament at the crack tip $b$ for different values of applied loads $\sigma_{13}^{\infty}$

Additional numerical analysis showed that the shear stress $\sigma_{13}(x_1, 0)$ in the neighborhood to the right of the crack depends very slightly on the compressive loading $\sigma_{33}^{\infty}$.

Figures 5 and 6 show, respectively, the variation of the relative contact zone length $\lambda_0$ and the ERR $G_0$ for various locations of the applied concentrated loading, defined by parameter $\theta$. Again, the positions have been chosen in the left half of the cracked region in order to minimize the effect of the oscillating singularity at the left crack tip on the contact zone at the right crack tip. The results are obtained for different normal loads $\sigma_{33}^{\infty} = -4\,\text{MPa}$ (line 1), $\sigma_{33}^{\infty} = -8\,\text{MPa}$ (line 2) and $\sigma_{33}^{\infty} = -12\,\text{MPa}$ (line 3) with fixed shear load $\sigma_{13}^{\infty} = -10\,\text{MPa}$. It follows from the presented figures that the variation of the position of the concentrated force can retard or enhance the relative contact zone length and the stress level in the vicinity of the crack tip. An increase in parameter $\theta$ (i.e., decrease in $d$) leads to an increase in the relative contact zone length $\lambda_0$ and a decrease in the energy release rate $G_0$. Thus, according to the maximum energy release rate criterion, the closer the applied concentrated mechanical load approaches the left crack tip, the easier growth and propagation of the right crack tip will be.

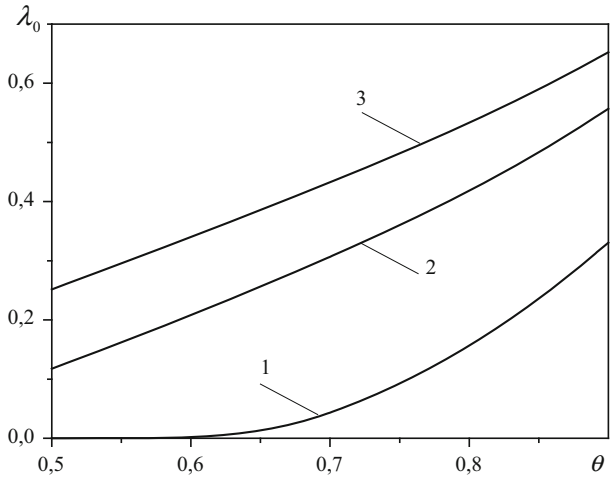


**Fig. 5** Dependencies of the relative contact zone length $\lambda_0$ with respect to the location of the applied concentrated loads $\theta$ for different values of normal loads $\sigma_{33}^{\infty}$

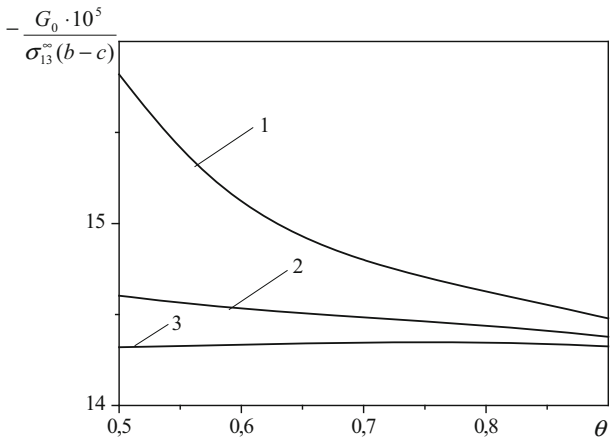


**Fig. 6** Dependencies of the ERR $G_0$ with respect to the location of the applied concentrated loads $\theta$ for different values of normal loads $\sigma_{33}^{\infty}$

## 8 Conclusions

A crack between two piezoelectric materials under concentrated loading applied to the crack faces and remote mixed-mode loading is considered. It is assumed that in this case there are open and closed parts of the crack, and frictionless crack faces contact is adopted in its closed part.

Using representations of displacements and stresses by means of piecewise analytic functions, the problem is reduced to a combined Dirichlet–Riemann boundary value problem. Using the exact analytical solution of this problem, the analytical expressions for the displacement jumps and for the stresses along the interface are presented. The stress intensity factors and the energy release rates are found in closed form. The contact zone length in a Comninou's sense has been derived as a particular case of the obtained solution. Namely, the transcendental equation for the determination of this length has been obtained.

The numerical results are presented in the form of Table 1 and Figs. 2, 3, 4, 5 and 6. These results show that a zone of open crack faces is present for all considered loadings. For a compressive normal stress, the shear stress plays the determinative role concerning the possibility of crack growth. At the same time, the stress intensity factor of the shear stress and the energy release rate depend very slightly on the magnitude of the compressive loading. The influence of the magnitude and locations of the applied concentrated loading upon the contact zone length and the associated fracture mechanical parameters has been demonstrated. It was shown that an increase in the distance from the concentrated force to the crack tip leads to an increase in the relative contact zone length and a decrease in the energy release rate.

**Acknowledgments** The author V. Govorukha would like to express his gratitude for the support of the Alexander von Humboldt Foundation (Germany).

## References

1. Sosa, H.: Plane problems in piezoelectric media with defects. Int. J. Solids Struct. **28**, 491–505 (1991)
2. Shindo, Y., Tanaka, K., Narita, F.: Singular stress and electric fields of a piezoelectric ceramic strip with a finite crack under longitudinal shear. Acta Mech. **120**, 31–45 (1997)
3. Pak, Y.E.: Linear electro-elastic fracture mechanics of piezoelectric materials. Int. J. Fract. **54**, 79–100 (1992)
4. Kuna, M.: Finite element analyses of crack problem in piezoelectric structures. Comput. Mater. Sci. **13**, 67–80 (1998)
5. Gao, C.F., Fan, W.X.: Exact solution for the plane problem in piezoelectric materials with an elliptic hole or a crack. Int. J. Solids Struct. **36**, 2527–2540 (1999)
6. Xu, X.L., Rajapakse, R.K.N.D.: On a plane crack in piezoelectric solids. Int. J. Solids Struct. **38**, 7643–7658 (2001)
7. McMeeking, R.M.: The energy release rate for a Griffith crack in a piezoelectric material. Eng. Fract. Mech. **71**, 1149–1163 (2004)
8. Parton, V.Z.: Fracture mechanics of piezoelectric materials. Acta Astronaut. **3**, 671–683 (1976)
9. Kuo, C.M., Barnett, D.M. : Stress singularities of interfacial cracks in bonded piezoelectric half-spaces. In: Wu, J.J., Ting, T.C.T., Barnett, D.M. (eds.) Modern Theory of Anisotropic Elasticity and Applications, pp. 33–50. SIAM, Philadelphia (1991)
10. Suo, Z., Kuo, C.M., Barnet, D.M., Willis, J.R.: Fracture mechanics for piezoelectric ceramics. J. Mech. Phys. Solids **40**, 739–765 (1992)
11. Gao, C.F., Haeusler, C., Balke, H.: Periodic permeable interface cracks in piezoelectric materials. Int. J. Solids Struct. **41**, 323–335 (2004)
12. Ma, L.F., Chen, Y.H.: Weight functions for interface cracks in dissimilar anisotropic piezoelectric materials. Int. J. Fract. **110**, 263–279 (2001)
13. Beom, H.G.: Permeable cracks between two dissimilar piezoelectric materials. Int. J. Solids Struct. **40**, 6669–6679 (2003)
14. Li, Q., Chen, Y.H.: Solution of a semi-permeable interface crack in dissimilar piezoelectric materials. J. Appl. Mech. **74**, 833–844 (2007)
15. Beom, H.G., Atluri, S.N.: Near-tip fields and intensity factors for interfacial cracks in dissimilar anisotropic piezoelectric media. Int. J. Fract. **75**, 163–183 (1996)
16. Ou, Z.C., Wu, X.: On the crack-tip stress singularity of interfacial cracks in transversely isotropic piezoelectric bimaterials. Int. J. Solids Struct. **40**, 7499–7511 (2003)
17. Qin, Q.H., Yu, S.W.: An arbitrarily-oriented plane crack terminating at the interface between dissimilar piezoelectric materials. Int. J. Solids Struct. **34**, 581–590 (1997)
18. Williams, M.L.: The stresses around a fault or cracks in dissimilar media. Bull. Seismol. Soc. Am. **49**, 199–204 (1959)
19. Comninou, M.: The interface crack. J. Appl. Mech. **44**, 631–636 (1977)
20. Atkinson, C.: The interface crack with a contact zone (an analytical treatment). Int. J. Fract. **18**, 161–177 (1982)
21. Simonov, I.V.: An interface crack in an inhomogeneous stress field. Int. J. Fract. **46**, 223–235 (1990)
22. Gautesen, A.K., Dundurs, J.: The interface crack under a combined loading. J. Appl. Mech. **55**, 580–586 (1988)
23. Loboda, V.V.: The quasi-invariant in the theory of interface crack. Eng. Fract. Mech. **44**, 573–580 (1993)
24. Qin, Q.H., Mai, Y.W.: A closed crack tip model for interface cracks in thermopiezoelectric materials. Int. J. Solids Struct. **36**, 2463–2479 (1999)
25. Herrmann, K.P., Loboda, V.V., Khodanen, T.V.: An interface crack with contact zones in a piezoelectric/piezomagnetic bimaterial. Arch. Appl. Mech. **80**, 651–670 (2010)
26. Feng, W.J., Ma, P., Su, R.K.L.: An electrically impermeable and magnetically permeable interface crack with a contact zone in magnetoelectroelastic bimaterials under a thermal flux and magnetoelectromechanical loads. Int. J. Solids Struct. **49**, 3472–3483 (2012)
27. Herrmann, K.P., Loboda, K.P.: Fracture-mechanical assessment of electrically permeable interface cracks in piezoelectric bimaterials by consideration of various contact zone models. Arch. Appl. Mech. **70**, 127–143 (2000)
28. Herrmann, K.P., Loboda, V.V., Govorukha, V.B.: On contact zone models for an electrically impermeable interface crack in a piezoelectric bimaterial. Int. J. Fract. **111**, 203–227 (2001)
29. Govorukha, V., Kamlah, M.: On contact zone models for an electrically limited permeable interface crack in a piezoelectric bimaterial. Int. J. Fract. **164**, 133–146 (2010)
30. Comninou, M., Schmueser, D.: The interface crack in a combined tension-compression and shear field. J. Appl. Mech. **46**, 345–348 (1979)
31. Chen, Y.H., Han, J.J.: Macrocrack-microcrack interaction in piezoelectric materials, Part I: basic formulations and J-analysis. J. Appl. Mech. **66**, 514–521 (1999)
32. Hou, P.F., Ding, H.J., Guan, F.L.: Point forces and point charge applied to a circular crack in transversely isotropic piezoelectric space. Theor. Appl. Fract. Mech. **36**, 245–262 (2001)
33. Parton, V.Z., Kudryavtsev, B.A.: Electromagnetoelasticity. Gordon and Breach Science Publishers, New York (1988)
34. Nahmein, E.L., Nuller, B.M.: Contact of an elastic half plane and a particularly unbonded stamp. Prikl. Math. Mech. **50**, 663–678 (1986)
35. Gakhov, F.D.: Boundary Value Problems. Pergamon Press, Oxford (1966)
36. Park, S.B., Sun, C.T.: Fracture criteria for piezoelectric ceramics. J. Am. Ceram. Soc. **78**, 1475–1480 (1995)